Modeling two-dimensional solid-phase epitaxial regrowth using level set methods

S. Morarka,[1,a)] N. G. Rudawski,[2] M. E. Law,[1] K. S. Jones,[2] and R. G. Elliman[3]
[1]*Department of Electrical and Computer Engineering, University of Florida, Gainesville, Florida 32611-6200, USA*
[2]*Department of Materials Science and Engineering, University of Florida, Gainesville, Florida 32611-6400, USA*
[3]*Department of Electronic Materials Engineering, Research School of Physical Sciences and Engineering, Australian National University, Canberra, Australian Capital Territory 0200, Australia*

(Received 21 November 2008; accepted 11 January 2009; published online 3 March 2009)

Modeling the two-dimensional (2D) solid-phase epitaxial regrowth (SPER) of amorphized Si (variously referred to as solid-phase epitaxial growth, solid-phase epitaxy, solid-phase epitaxial crystallization, and solid-phase epitaxial recrystallization) has become important in light of recent studies which have indicated that relative differences in the velocities of regrowth fronts with different crystallographic orientations can lead to the formation of device degrading mask edge defects. Here, a 2D SPER model that uses level set techniques as implemented in the Florida object oriented process simulator to propagate regrowth fronts with variable crystallographic orientation (patterned material) is presented. Apart from the inherent orientation dependence of the SPER velocity, it is established that regrowth interface curvature significantly affects the regrowth velocity. Specifically, by modeling the local SPER velocity as being linearly dependent on the local regrowth interface curvature, data acquired from transmission electron microscopy experiments matches reasonably well with simulations, thus providing a stable model for simulating 2D regrowth and mask edge defect formation in Si. © *2009 American Institute of Physics*. [DOI: 10.1063/1.3082086]

I. INTRODUCTION

Solid-phase epitaxial regrowth (SPER) of Si occurs during formation of source and drain regions of complementary metal-oxide-semiconductor (CMOS) devices, in particular, during creation of ultrashallow junctions with high dopant activation.[1,2] SPER during CMOS device fabrication is also believed to be a key component of stress memorization techniques used to enhance channel mobility.[3,4]

The macroscopic velocity, v, of an interface between amorphous (α) and crystalline (c) phases (also referred to as the SPER or regrowth front/interface) is known to be a thermally activated process with an activation energy of ~2.7 eV.[5,6] Additionally, SPER is affected by the crystal orientation of α-Si/c-Si interface,[7] impurities,[8–14] and applied mechanical stress.[15–29] It is also known that SPER is inhibited at the point of contact between the regrowth front and Si_3N_4 or SiO_2.[30] However, since SPER is of the most technological relevance in source and drain regions generated from patterned α-Si regions with variable crystallographic orientation of the regrowth front, it cannot be modeled as a one-dimensional (1D) process. SPER, in the most general sense is a three-dimensional (3D) process but in case of one of the dimensions of the structure being very long, it effectively can be treated as a two-dimensional (2D) process. In our study, the pattern is made up of long lines with finite spacing which, in terms of CMOS devices, is effectively equivalent to assuming that the "width" (this corresponds to the dimension into the page in all of the figures) of the transistor is very long, which is a good assumption for many devices. For purposes of simplicity we have not investigated the 3D case although it may be relevant in certain situations.

The substrate orientation dependence of SPER is therefore very important to consider. The normalized regrowth velocity, $f(\theta)$, as a function of the substrate orientation angle from [001] toward [110] (θ) was measured by Csepregi *et al.*[7] as shown in Fig. 1 with the fastest regrowth velocity along [001] [corresponding to $f(\theta)=1.0$]. Thus, v as a function of θ, is given by

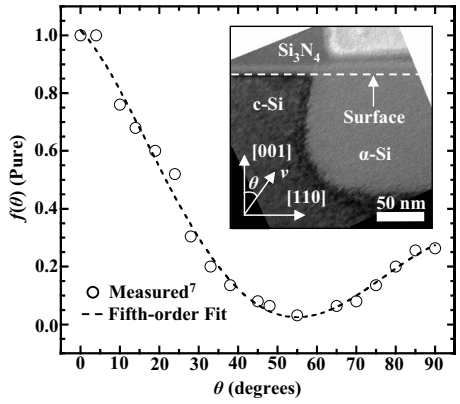

FIG. 1. The normalized SPER velocity, $f(\theta)$, as a function of the substrate orientation angle from [001] toward [110], θ, as measured by Csepregi *et al.* (Ref. 7) The inset shows an XTEM micrograph of a typical 2D structure where the SPER process occurs.

[a)]Author to whom correspondence should be addressed. Electronic mail: saurabhm@ufl.edu.

$$v(\theta) = v_{[001]} f(\theta), \quad (1)$$

where $v_{[001]}$ is the value of v along [001] and $f(\theta)$ is temperature independent and accurately fit using a least-squares fifth-order polynomial. The [001] regrowth velocity is ~25 times faster than the slowest regrowth direction of [111] and almost ~4 times faster than the [110] direction. This orientation dependence was also observed in studies using patterned amorphized wafers.[31–42]

Previous attempts[43] to model and simulate the orientation dependence of SPER in the patterned amorphized regions have been made but have not been extended to initial α-c interfaces with any shape other than rectilinear. This somewhat limits the capability of prior models in predicting SPER evolution for different types of initial α-c interfaces and makes it difficult to gain further insight into the nature of regrowth.

In particular, predicting and modeling the evolution of 2D SPER in patterned amorphized regions is very important since mask edge defects are known to occur during this process.[31–42] It is believed that mask edge defects are caused by the regrowth dependence on substrate orientation.[31,41] Specifically, since the [001] and [110] directions are much faster than the [111] direction, a portion of the α-Si near the [111] fronts can become encompassed and "pinched off" from the remaining α-Si layer via the regrowth interface collapsing upon itself. Saenger *et al.*[42] showed that the defects were created along ⟨111⟩-type directions in both (001) and (011) wafers which suggests that impingement of the [111] front is primarily responsible for mask edge defect formation.

Thus, the goal of this work is to study and simulate the 2D SPER process in different types of structures to gain greater insight into the nature of regrowth and to allow greater understanding and predictability of the mask edge defect nucleation process.

II. EXPERIMENTAL PROCEDURES AND LEVEL SET MODELING

For this work, 750-μm thick (001) Si wafers were used. Masked regions consisted of lines ~0.5 μm wide aligned along ⟨110⟩ in-plane directions with 150 nm of Si_3N_4 (~1 GPa intrinsic tensile stress) on ~10 nm of SiO_2 separated by ~0.5 μm wide unmasked area between adjacent lines. Some samples were Si^+ implanted at 20 and 60 keV with doses of 1×10^{15} cm^{-2}. This produced an α-Si layer ~120 nm deep with a rounded α-c interface under the mask edge as shown in the cross-sectional transmission electron microscopy (XTEM) image presented in Fig. 2(a). From the work of Burbure *et al.*,[30] it is expected that the regrowth interface contacting the SiO_2 layer just under the masking will constrict SPER at this point. Hence, these samples are referred to as having the regrowth interface subjected to surface pinning.

Another set of samples was Si^+ implanted at 20, 60, and 160 keV with doses of 1×10^{15}, 1×10^{15}, and 3×10^{15} cm^{-2} to generate an undulating α-Si layer ~100 nm thick under the masking and ~200 nm thick in the open areas as shown in Fig. 4(a). In this case, the regrowth interface is not in contact with any portion of the surface and is therefore not subjected to any surface pinning.[30] Thus, these sample are referred to as being without regrowth interface pinning.

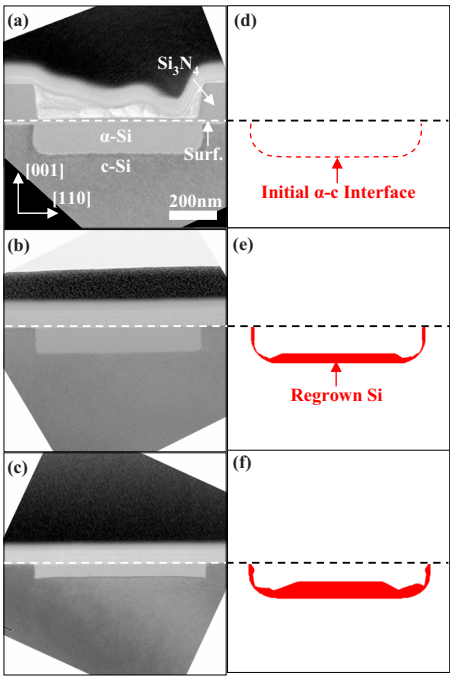

FIG. 2. (Color online) The observed and curvature-free simulated 2D SPER process in a structure with α-c interfacial pinning at the surface at $T=500$ °C: XTEM images of the structure (a) as-implanted, (b) after 1 h of annealing, and (c) after 2 h of annealing. Level set simulations of the structure evolution using only regrowth orientation dependence [Eq. (1)] (d) as-implanted, (e) after 1 h of annealing, and (f) after 2 h of annealing.

The samples were annealed at temperatures of $T=500$–575 °C in N_2 ambient for times of 0.5–10.0 h. Anneal times were chosen to see different points during the regrowth process when the regrowth evolution showed important changes. The samples with interfacial pinning had the Si_3N_4 removed prior to annealing, while samples without interfacial pinning were annealed with and without the Si_3N_4 intact. In the latter case, the presence of the Si_3N_4 did not greatly alter the regrowth process and only the samples with the Si_3N_4 are reported for clarity. XTEM imaging was used to image the 2D SPER process with XTEM specimens prepared via focused ion beam milling.

The 2D SPER process was modeled using level set techniques and implemented in the Florida object oriented process simulator (FLOOPS).[44] Level set simulations have previously been used in etching and deposition simulation and can be readily used to track the velocity of a moving interface with the level set method being very stable regarding the propagation of sharp corners of the interface or merging of two fronts.[45] In simulating SPER, the interface of interest is the α-c interface. More details about level set techniques are presented elsewhere.[45,46] Additionally, the use of FLOOPS provides the advantage of being able to link the regrowth model to the prior diffusion models used in process simulation.[44]

III. RESULTS AND DISCUSSION

Figures 2(a)–2(c) present XTEM images of the 2D SPER process at $T=500$ °C in samples with surface regrowth interface pinning. After annealing for 1 h, the α-c interface has taken on a rectangular shape with the initially round corner area becoming very sharp as shown in Fig. 2(b). After annealing for 2 h, the regrowth interface near the corner regions has further sharpened as shown in Fig. 2(c). The level set SPER simulations after 1 and 2 h of annealing based on the orientation dependent regrowth velocity from Eq. (1) (using $v_{[001]}=27$ nm/h as reported[5,6]) are shown in Figs. 2(e) and 2(f), respectively, with $v=0$ specified for the point at which the interface contacts the SiO_2 layer. It is evident from Fig. 2 that the portions of the regrowth fronts near the corner regions do not match the XTEM images. Specifically, it appears regrowth along [111] is slower in the simulations than actually observed. Furthermore, enhancing the relative regrowth velocity of the [111] direction from ~25 times slower than [001] to ~15 times slower (as per results from Csepregi *et al.*[7] who indicated two different velocities for [111] SPER) did not appreciably change the simulated SPER process (not presented). Thus, it appears that differences in the relative regrowth rates of different crystallographic fronts cannot entirely account for the observed SPER evolution.

Drosd *et al.*[47] showed that the local interfacial curvature, κ, affects the regrowth rate along [111] and attributed this to the fact that (111) interface is atomically smooth and should propagate by nucleation and growth of atomic ledges. Hence, if a portion of c-Si is encompassed by α-Si (negative or convex curvature), SPER should be retarded, while if the α-Si is encompassed by c-Si (positive or concave curvature), as shown in Figs. 1 and 2, SPER should be enhanced. Furthermore, it was shown that when the radius of curvature, $r=1/\kappa$, was below ~20 μm, a measurable increase in regrowth rate occurred.[47] In the presented cases, the growth interface has portions where $r\sim 0.1$ μm

Thus, Eq. (1) was modified to be linearly dependent on interfacial curvature via

$$v(\theta,\kappa)=v_{[001]}f(\theta)(1+A\kappa), \tag{2}$$

where A is a constant with units of length. For the presented work $A=2.0\times10^{-7}$ cm was used. Equation (2) was used for level set simulation of the 2D SPER process at $T=500$ °C in samples with surface regrowth interface pinning as shown in Fig. 3. After annealing for 1 h, the XTEM image and level set simulation of SPER shown in Figs. 3(a) and 3(d) are in good agreement. This is also the case after annealing for 2 h as shown in Figs. 3(b) and 3(e) as well as after annealing for 4 h as shown in Figs. 3(c) and 3(f).

The implication of Eq. (2) is that portions of the regrowth interface with $\kappa>0$ ($\kappa<0$) should have enhanced (reduced) velocity. It is evident from Fig. 3 (surface interfacial pinning) that Eq. (2) appears to be valid for the case of $\kappa\geq0$ since most of the regrowth front is of this type. However, the converse is not necessarily evident.

To test the influence of $\kappa<0$ on the 2D SPER process, structures lacking interfacial pinning, shown in Fig. 4, were annealed at $T=500$ °C up to 10 h. It can be readily seen that both concave and convex portions of the regrowth interface exist in this structure. After annealing for 2.5 h, shown in Fig. 4(b), the concave portion of the interface becomes sharp while the convex part begins to flatten. After annealing for 5.0 h, as presented in Fig. 4(c), mask edge defects started to form as the corner region of the interface has impinged upon itself. Following annealing for 10.0 h, shown in Fig. 4(d), two triangular α-Si regions remain under the mask edge. Level set simulation of the 2D SPER process at $T=500$ °C in structures without interfacial pinning was done assuming Eq. (2) to be valid. In all cases of annealing, the simulated SPER process, shown in Figs. 4(f)–4(h), matches very well with the corresponding XTEM images, shown in Figs. 4(b)–4(d).

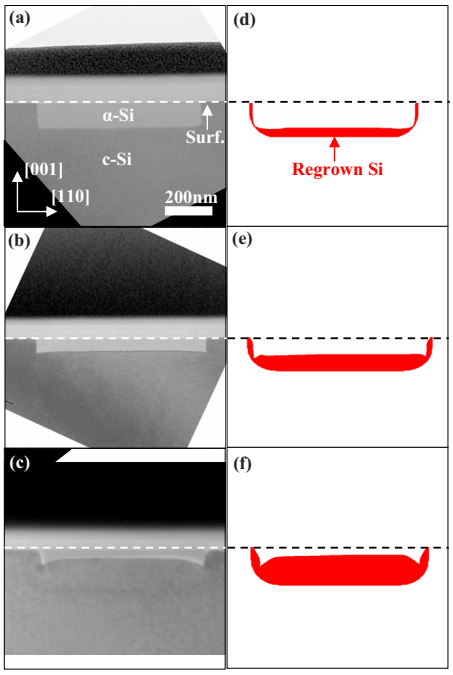

FIG. 3. (Color online) The observed and curvature-included simulated 2D SPER process in a structure with α-c interfacial pinning at the surface at $T=500$ °C: XTEM images of the structure after annealing for (a) 1, (b) 2, and (c) 4 h. Level set simulations of the structure evolution using both regrowth orientation and interfacial curvature dependence [Eq. (2)] for (d) 1, (e) 2, and (f) 4 h.

The 2D SPER process in samples without interface pinning was also examined at $T=525$ and 575 °C using XTEM (not presented). In these cases, the SPER evolution was faster (as expected due to the thermally activated[5,6] nature of SPER) but the shape of the evolving regrowth interface was nearly identical to the case of $T=500$ °C. The implication of this is that the apparent influence of interfacial curvature on SPER is nearly temperature independent.

Figure 5 shows the simulated 2D SPER process in samples with surface interface pinning at different initial values of r under the mask edge with the same initial α-Si thickness of ~150 nm. As r increases, it is more difficult for the regrowth interface to collapse upon itself (and thus form mask edge defects). In fact, this prediction is verified by a prior study in which a sine-wave-type regrowth interface with very low amplitude completely flattened after sufficient

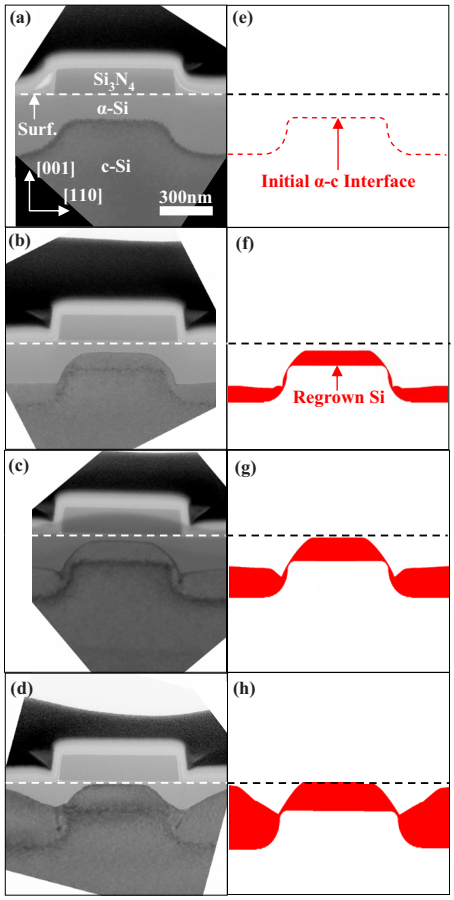

FIG. 4. (Color online) The observed and curvature-included simulated 2D SPER process in a structure without α-c interfacial pinning at the surface at $T=500$ °C: XTEM images of the structure (a) as-implanted, (b) after annealing for 2.5 h, (c) after annealing for 5.0 h, and (d) after annealing for 10.0 h. Level set simulations of the structure evolution using both regrowth orientation and interfacial curvature dependence [Eq. (2)] (e) as-implanted, (f) after annealing for 2.5 h, (g) after annealing for 5.0 h, and (h) after annealing for 10.0 h.

annealing and exhibited no defects.[24] Thus, the model can be used to successfully predict the formation of mask edge defects depending on the initial α-c interface shape.

Prior simulation work by Phan *et al.*[43] advanced that the curvature of a regrowth interface does not influence the activation barrier for SPER. Additionally, Phan *et al.*[43] addressed the influence of curvature on the driving force for recrystallization and determined it produced a negligible impact on the regrowth kinetics. However, although thermodynamic considerations may be negligible, it does appear from the work presented herein that interfacial curvature is altering SPER kinetics. Perhaps no curvature effect was observed because of the relatively planar nature of the structures used in the prior work.

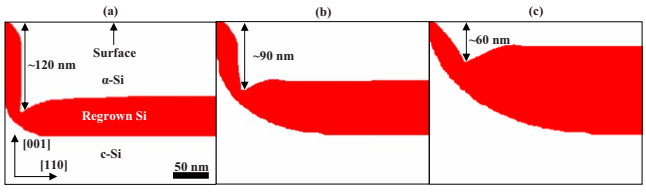

FIG. 5. (Color online) The effect of initial α-c interface curvature near the corner region on the level set simulations using both regrowth orientation and interfacial curvature dependence [Eq. (2)] of the 2D SPER process in a structure with α-c interfacial pinning at the surface: $r=$(a) 40, (b) 80, and (c) 120 nm.

In terms of explaining the apparent linear dependence of the SPER velocity with interfacial curvature observed herein, it is useful to consider the likelihood of the α-c interface having an inherent amount of internal tension as was suggested by others.[48,49] Thus, it is foreseeable that portions of an interface with nonzero curvature would experience localized stresses much different from the case of an interface with zero curvature. Furthermore, it has been well established that stress on the regrowth interface can significantly alter the kinetics of SPER due to changes in volume associated with the process.[15–29] Hence, it is possible that interfacial curvature is influencing the localized stress states on the interface and altering regrowth.

IV. CONCLUSIONS

In summary, the 2D solid-phase epitaxial regrowth process of Si was studied using transmission electron microscopy and modeled using level set methods. Initially, only the substrate orientation dependence of regrowth was considered in simulations, but this approach failed to accurately predict the evolution of the regrowth process in structures where the regrowth interface was pinned at the surface. However, modifying the orientation dependent regrowth model to also be linearly dependent on the local interface curvature did accurately account for the regrowth evolution. This same curvature dependence was also successful in predicting the regrowth evolution in structures where regrowth interface pinning was not present. Interestingly, the apparent linear dependence of regrowth kinetics on interface curvature was temperature insensitive. Physically, it is still unclear why the regrowth velocity would be linearly dependent on interface curvature, but this may be possibly related to tension generated in the regrowth interface.

ACKNOWLEDGMENTS

The authors acknowledge the Semiconductor Research Corporation for funding this work. The Major Analytical Instrumentation Center at the University of Florida is acknowledged for use of the focused ion beam and transmission electron microscopy facilities.

[1] A. Bousetta, J. A. Vandenberg, R. Valizadeh, D. G. Armour, and P. C. Zalm, Nucl. Instrum. Methods Phys. Res. B **55**, 565 (1991).
[2] J. J. Hamilton, E. J. H. Collart, B. Colombeau, C. Jeynes, M. Bersani, D. Giubertoni, J. A. Sharp, N. E. B. Cowern, and K. J. Kirkby, Nucl. Instrum. Methods Phys. Res. B **237**, 107 (2005).
[3] P. Morin, E. Mastromatteo, C. Chaton, C. Ortolland, and F. Arnaud, Mater. Sci. Eng., B **135**, 215 (2006).
[4] K. Ota, K. Sugihara, H. Sayama, T. Uchida, H. Oda, T. Eimori, H. Morimoto and Y. Inoue, Tech. Dig. - Int. Electron Devices Meet. **2002**, 27.
[5] G. A. Olson and J. A. Roth, Mater. Sci. Rep. **3**, 1 (1988).
[6] J. A. Roth, G. L. Olson, D. C. Jacobson, and J. M. Poate, Appl. Phys. Lett. **57**, 1340 (1990).
[7] L. Csepregi, E. F. Kennedy, J. W. Mayer, and T. W. Sigmon, J. Appl. Phys. **49**, 3906 (1978).
[8] L. Csepregi, E. F. Kennedy, T. J. Gallagher, J. W. Mayer, and T. W. Sigmon, Appl. Phys. (Berlin) **48**, 4234 (1977).
[9] E. F. Kennedy, L. Csepregi, J. W. Mayer, and T. W. Sigmon, J. Appl. Phys. **48**, 4241 (1977).

[10]I. Suni, G. Göltz, M. G. Grimaldi, M.-A. Nicolet, and S. S. Lau, Appl. Phys. Lett. **40**, 269 (1982).
[11]J. S. Williams and R. G. Elliman, Phys. Rev. Lett. **51**, 1069 (1983).
[12]W. O. Adekoya, M. Hage-Ali, J. C. Muller, and P. Siffert, J. Appl. Phys. **64**, 666 (1988).
[13]J. C. McCallum, Nucl. Instrum. Methods Phys. Res. B **148**, 350 (1999).
[14]B. C. Ishitani and J. C. McCallum, Phys. Rev. B **76**, 045206 (2007).
[15]E. Nygren, M. J. Aziz, and D. Turnbull, Appl. Phys. Lett. **47**, 232 (1985).
[16]G.-Q. Lu, E. Nygren, M. J. Aziz, D. Turnbull, and C. W. White, Appl. Phys. Lett. **54**, 2583 (1989).
[17]G.-Q. Lu, E. Nygren, and M. J. Aziz, J. Appl. Phys. **70**, 5232 (1991).
[18]T. K. Chaki, Philos. Mag. Lett. **63**, 303 (1991).
[19]K. L. Saenger, K. E. Fogel, J. A. Ott, J. P. de Souza, and C. E. Murray, Appl. Phys. Lett. **92**, 124103 (2008).
[20]M. J. Aziz, P. C. Sabin, and G.-Q. Lu, Phys. Rev. B **44**, 9812 (1991).
[21]W. Barvosa-Carter and M. J. Aziz, Appl. Phys. Lett. **79**, 356 (2001).
[22]W. Barvosa-Carter, M. J. Aziz, A.-V. Phan, T. Kaplan, and L. J. Gray, J. Appl. Phys. **96**, 5462 (2004).
[23]W. Barvosa-Carter, M. J. Aziz, L. J. Gray, and T. Kaplan, Phys. Rev. Lett. **81**, 1445 (1998).
[24]J. F. Sage, W. Barvosa-Carter, and M. J. Aziz, Appl. Phys. Lett. **77**, 516 (2000).
[25]N. G. Rudawski, K. S. Jones, and R. Gwilliam, Appl. Phys. Lett. **91**, 172103 (2007).
[26]N. G. Rudawski, K. S. Jones, and R. Gwilliam, Phys. Rev. Lett. **100**, 165501 (2008).
[27]N. G. Rudawski, K. S. Jones, and R. Gwilliam Mater. Sci. Eng. R. **61**, 40 (2008).
[28]N. G. Rudawski, K. S. Jones, and R. Gwilliam, Appl. Phys. Lett. **92**, 232110 (2008).
[29]N. G. Rudawski, K. S. Jones, and R. Gwilliam, J. Mater. Res. **24**. 305 (2009).
[30]N. Burbure, N. G. Rudawski, and K. S. Jones, Electrochem. Solid-State Lett. **10**, H184 (2007).
[31]H. Cerva and K.-H. Küsters, J. Appl. Phys. **66**, 4723 (1989).
[32]H. Cerva and W. Bergholz, J. Electrochem. Soc. **140**, 780 (1993).
[33]H. Cerva, Defect Diffus. Forum **148**, 103 (1997).
[34]Y. G. Shin, J. Y. Lee, M. H. Park, and H. K. Kang, J. Cryst. Growth **233**, 673 (2001).
[35]Y. G. Shin, J. Y. Lee, M. H. Park, and H. K. Kang, J. Cryst. Growth **231**, 107 (2001).
[36]Y. G. Shin, J. Y. Lee, M. H. Park, and H. K. Kang, Jpn. J. Appl. Phys. **40**, 6192 (2001).
[37]C. Ross and K. S. Jones, Mater. Res. Soc. Symp. Proc. **810**, C10.4 (2004).
[38]C. R. Olson, E. Kuryliw, B. E. Jones, and K. S. Jones, J. Vac. Sci. Technol. B **24**, 446 (2006).
[39]N. G. Rudawski, K. N. Siebein, and K. S. Jones, Appl. Phys. Lett. **89**, 082107 (2006).
[40]N. G. Rudawski, K. S. Jones, and R. G. Elliman, J. Vac. Sci. Technol. B **26**, 435 (2008).
[41]N. G. Rudawski, K. S. Jones, S. Morarka, M. E. Law, and R. G. Elliman, J. Appl. Phys. (submitted).
[42]K. L. Saenger, J. P. de Souza, K. E. Fogel, J. A. Ott, C. Y. Sung, D. K. Sadana, and H. Yin, J. Appl. Phys. **101**, 104908 (2007).
[43]A.-V. Phan, T. Kaplan, L. J. Gray, D. Adalsteinsson, J. A. Sethian, W. Barvosa-Carter, and M. J. Aziz, Modell. Simul. Mater. Sci. Eng. **9**, 309 (2001).
[44]M. E. Law and S. M. Cea, Comput. Mater. Sci. **12**, 289 (1998).
[45]J. A. Sethian, *Level Set Methods and Fast Marching Methods* (Cambridge University Press, New York, 1999).
[46]S. Morarka, N. G. Rudawski, and M. E. Law, J. Vac. Sci. Technol. B **26**, 357 (2008).
[47]B. Drosd and J. Washburn, J. Appl. Phys. **51**, 4106 (1980).
[48]N. Bernstein, M. J. Aziz, and E. Kaxiras, Phys. Rev. B **58**, 4579 (1998).
[49]F. Spaepen, Acta Metall. **26**, 1167 (1978).